Neurobiology of Disease 44 (2011) 9–18

Contents lists available at ScienceDirect

Neurobiology of Disease

journal homepage: www.elsevier.com/locate/ynbdi

Evaluation of spontaneous propulsive movement as a screening tool to detect rescue of Parkinsonism phenotypes in zebrafish models

Thomas C. Farrell [a,b], Clinton L. Cario [a,b], Chiara Milanese [a,b,g], Andreas Vogt [c,d], Jong-Hyeon Jeong [f], Edward A. Burton [a,b,e,h,i,*]

[a] Pittsburgh Institute for Neurodegenerative Diseases, University of Pittsburgh, School of Medicine, Pittsburgh, PA, USA
[b] Department of Neurology, University of Pittsburgh, School of Medicine, Pittsburgh, PA, USA
[c] Department of Computational and Systems Biology, University of Pittsburgh, School of Medicine, Pittsburgh, PA, USA
[d] University of Pittsburgh Drug Discovery Institute, University of Pittsburgh, School of Medicine, Pittsburgh, PA, USA
[e] Department of Microbiology and Molecular Genetics, University of Pittsburgh, School of Medicine, Pittsburgh, PA, USA
[f] Department of Biostatistics, University of Pittsburgh, Graduate School of Public Health, Pittsburgh, PA, USA
[g] RIMED Foundation, Palermo, Italy
[h] Geriatric Research, Education and Clinical Center, Pittsburgh VA Healthcare System, Pittsburgh, PA, USA
[i] Department of Neurology, Pittsburgh VA Healthcare System, Pittsburgh, PA, USA

ARTICLE INFO

Article history:
Received 23 January 2011
Revised 23 May 2011
Accepted 25 May 2011
Available online 6 June 2011

Keywords:
Zebrafish
Parkinsonism
Motor function
Dopamine
MPP^+
Chlorpromazine
Haloperidol
Apomorphine
Ropnirole
Spontaneous movement
Automated behavior measurement
Drug discovery

ABSTRACT

Zebrafish models of human neuropsychiatric diseases offer opportunities to identify novel therapeutic targets and treatments through phenotype-based genetic or chemical modifier screens. In order to develop an assay to detect rescue of zebrafish models of Parkinsonism, we characterized spontaneous zebrafish larval motor behavior from 3 to 9 days post fertilization in a microtiter plate format suitable for screening, and clarified the role of dopaminergic signaling in its regulation. The proportion of time that larvae spent moving increased progressively between 3 and 9 dpf, whereas their active velocity decreased between 5 and 6 dpf as sporadic burst movements gave way to a more mature beat-and-glide pattern. Spontaneous movement varied between larvae and during the course of recordings as a result of intrinsic larval factors including genetic background. Variability decreased with age, such that small differences between groups of larvae exposed to different experimental conditions could be detected robustly by 6 to 7 dpf. Suppression of endogenous dopaminergic signaling by exposure to MPP^+, haloperidol or chlorpromazine reduced mean velocity by decreasing the frequency with which spontaneous movements were initiated, but did not alter active velocity. The variability of mean velocity assays could be reduced by analyzing groups of larvae for each data point, yielding acceptable screening window coefficients; the sample size required in each group was determined by the magnitude of the motor phenotype in different models. For chlorpromazine exposure, samples of four larvae allowed robust separation of treated and untreated data points ($Z = 0.42$), whereas the milder impairment provoked by MPP^+ necessitated groups of eight larvae in order to provide a useful discovery assay ($Z = 0.13$). Quantification of spontaneous larval movement offers a simple method to determine functional integrity of motor systems, and may be a useful tool to isolate novel molecular modulators of Parkinsonism phenotypes.

Published by Elsevier Inc.

Introduction

The long-term aim of our work is to develop improved treatments for neurological diseases associated with movement disorders. The zebrafish presents some methodological advantages as a tool to achieve this goal, including the unique applicability of high-throughput screening in a vertebrate model in vivo. Zebrafish larvae can be housed in 96-well plates, allowing libraries of small molecules to be assayed against phenotypes in order to identify compounds with disease-modifying potential (Zon and Peterson, 2005). Importantly, this can be carried out without making prior assumptions regarding drug targets, which might otherwise limit opportunities for discovery. Consequently, there is much interest in exploiting zebrafish models for the analysis of diseases and possible identification of new treatments. Phylogenetic conservation of many molecular, cellular and neuroanatomical features suggests that the zebrafish CNS presents a suitable biochemical and tissue environment to model human neurological disease, a prediction supported by recent studies showing that genetic or chemical manipulation of zebrafish can

* Corresponding author at: 7015 BST-3, 3501 Fifth Avenue, Pittsburgh PA 15217, USA. Fax: +1 412 648 9082.
E-mail address: eab25@pitt.edu (E.A. Burton).
Available online on ScienceDirect (www.sciencedirect.com).

0969-9961/$ – see front matter. Published by Elsevier Inc.
doi:10.1016/j.nbd.2011.05.016

recapitulate key features of relevant human disorders (Bandmann and Burton, 2010; Panula et al., 2010). Full exploitation of zebrafish neurological disease models for discovery of small molecule and genetic modifiers will be critically dependent on selection of appropriate phenotypic assays. In vivo models of neurological diseases have inherent advantages for modeling numerous aspects of disease pathogenesis, and also provide opportunities to use functional and behavioral assays as endpoints. The latter will be of particular importance in the study of diseases whose clinical manifestations are caused by disturbances in the physiology of neural circuits rather than neuronal cell loss, for example primary dystonia (Tanabe et al., 2009). Morphological end points might be uninformative for the analysis of these disorders, whereas physiological assays may be helpful.

Several different types of motor behavior can be quantified in zebrafish larvae, including spontaneous movement and evoked responses. The latter range in complexity, from reflex reactions to acoustic or cutaneous stimuli, to neurobehavioral traits relating to visual assessment of novel environmental cues or social behavior (Orger et al., 2004). Genetic (Muto et al., 2005; Peng et al., 2009) and chemical (Kokel et al., 2010; Rihel et al., 2010) screens relying on neurological or behavioral assays have recently been reported, demonstrating the feasibility of screening using functional end points. It is possible that a parallel approach might be used in genetic and chemical modifier screens to detect rescue of neurological phenotypes in disease models, raising the exciting prospect of phenotype-driven identification of novel therapeutic leads and drug targets in vivo. For the development of methodology to exploit zebrafish models of movement disorders for screening, we reasoned that an assay should be automated and applicable at larval time points at which high-throughput screening would be feasible, and at which pathogenesis might occur. In addition, the assay should quantify functions relevant to neural circuits implicated in pathogenesis, including the dopaminergic system that is centrally involved in many human movement disorders, and should yield quantitative data that could reliably detect a realistic level of partial phenotypic rescue.

After zebrafish embryos hatch, larval tail beating results in spontaneous propulsive movement (Drapeau et al., 2002). Previous work has shown that larval movement is modulated by dopaminergic function. The neurotoxins MPTP and MPP^+ reduced both the number of dopamine neurons (Bretaud et al., 2004; Lam et al., 2005; McKinley et al., 2005; Sallinen et al., 2008) and the total dopamine content (Sallinen et al., 2008) of larval zebrafish; exposure to these agents was associated with reduced motor activity, measured as the distance moved spontaneously over the course of an assay at 7 dpf (Sallinen et al., 2008), or as abnormalities of trunk movements in response to cutaneous stimuli in immobilized samples at 72 hpf (Lam et al., 2005). Similarly, dopamine D2 receptor antagonist drugs reduced displacement of 7 dpf and 14 dpf larvae over a 5-minute recording (Giacomini et al., 2006). These studies did not differentiate a hypokinetic phenotype (reduced number of movements) from a bradykinetic phenotype (executed movements are slower) in animals with impaired dopaminergic function. Furthermore, there is little published information on how spontaneous zebrafish motor behavior develops quantitatively during later larval stages, when neurodegenerative phenotypes realistically might become apparent, and little is known about how genetic background and environmental factors affect spontaneous movement and its variability. This information will be critical to understanding how spontaneous movement might be used as an assay for screening applications in Parkinsonism models. The purpose of this study was to quantify the development of spontaneous propulsive movement in zebrafish, to understand its sources of variability and the role of dopaminergic neurotransmission in its regulation, and to evaluate the suitability of spontaneous movement assays to detect rescue of motor function in a screening paradigm.

Materials and Methods

Zebrafish

Experiments were carried out in compliance with applicable regulations and approvals. Strain AB larvae were used for all experiments except the AB versus WIK comparison shown in Fig. 2C. Zebrafish embryos were raised in E3 medium (5 mM NaCl, 0.17 mM KCl, 0.33 mM $CaCl_2$, 0.33 mM $MgSO_4$, pH7.4) at 28.5 °C in a 14:10 h light:dark cycle (light cycles starts at 08:00; light color and intensity were identical to conditions used during recording). Medium was replaced daily, and was supplemented with methylene blue 0.00001% until 3 dpf. After 6 dpf, larvae were fed twice daily (Hatch Fry Encapsulon Grade 0, Argent Labs, Redmond WA). For movement analysis, larvae were carefully transferred into the E3-filled wells of multiwell plates using a large-bore Pasteur pipette with a flame-polished aperture of at least 4 mm to avoid mechanical damage. Larvae were acclimatized to wells for 30 min at 28.5 °C prior to recording. All recordings started at 09:00 (1 h after the lights came on). Chemicals were obtained from Sigma (St Louis, MO), catalog numbers: haloperidol, H1512; chlorpromazine hydrochloride, C8138; ropinirole hydrochloride, R2530; R-(−)-apomorphine hydrochloride hemihydrate, A4393; and 1-methyl-4-phenylpyridinium (MPP^+) iodide, D048. Exposure to chemicals was carried out by dissolving compounds in E3 buffer. For haloperidol, a stock solution was made in DMSO, and diluted in E3 buffer. The final concentration of DMSO was always below 0.5% v/v, which had no effect itself on measured movement parameters (not shown). Concentration–response curves for each compound were generated over a wide range of doses and are shown in Supplementary Fig. 4. The concentrations selected for the graphs shown in Figs. 3A and C represent doses that illustrate the trends discussed in the text. The concentration of MPP^+ selected for experiments shown in Figs. 3 and 4 was based on published data (Sallinen et al., 2008); larvae were raised in E3 buffer with 1 mM MPP^+ from days 2–6 and washed in E3 buffer prior to testing on day 7. All experiments were carried out in triplicate, with three independent biological replicates analyzed from different clutches of embryos on different days.

Video and analysis

A low temperature incubator (Thermo Precision # 3721) set to 28.5 °C was modified to house a fluorescent light source at the top of the chamber. Modified shelving housed microtiter plates below the light source allowing trans-illuminated wells to be visualized from underneath. Video recordings were made using a camcorder (Sony HDR-HC5) mounted on a tripod on an anti-vibration mat on the floor of the incubator, 70 cm below the plate. 96-well plates (CoStar, Corning, Lowell, MA) were milled to a depth of 10 mm to reduce shadow artifacts; areas between the wells were filled with black silica (Sylgard-186, Dow Chemicals) to assist object recognition and to prevent larvae in adjacent wells from acting as visual stimuli. Video was streamed at 2 frames/s, 720×406 pixels via IEEE1394 connection to a computer and then analyzed offline using custom software written using Matlab (Mathworks, Natick, MA) (Cario et al., 2011). The methodology is illustrated in Supplementary Fig. 1. Validation of video recording length, frame rate and resolution (4 h, 2 frames/s, 720×406 pixels) are shown in Supplementary Fig. 2. In each video frame, the software algorithm determined the coordinates of the larval centroid in each well, and then recorded centroid vector displacements between frames. After tracking was completed, for each larva simple calculations were carried out to determine: total displacement/recording time (mean velocity, V_M); the proportion of frames in which a movement was detected from the previous frame (% time moving, T%); and displacement/time spent moving (active velocity, V_A).

Statistical analysis

Measured kinetic parameters were normally distributed, as assessed by D'Agostino and Pearson's tests, and so parametric statistical analyses were used. Bar charts in Figs. 1A and B, 2C, 3A and C show mean values, error bars show the standard error of the mean. Coefficients of variation (C_V) are shown beneath each data point as standard deviation/mean. Pairwise comparisons shown in Figs. 2C, 3A, C were made using 2-tailed t-tests, assuming unequal variance and using Bonferroni correction for multiple comparisons. Variances between zebrafish strains shown in Fig. 2C were compared using F-test. Power analyses to determine detectable differences in Fig. 2D and optimal video recording length in Supplementary Fig. 2 were based on recorded values and standard deviations of V_M, V_A, T% at 7 dpf, assuming $\alpha = 0.05$ and $\beta = 0.9$. Variability attributable to intra-larval, inter-larval, and inter-assay differences in Fig. 2A was assessed using nested ANOVA. Assay window coefficient (Z factor) calculations were carried out as described (Zhang et al., 1999). For calculation in groups of 4 or 8 animals shown in Figs. 4A and B, groups were randomly assigned before the analysis was carried out in order to prevent introduction of biases from post-hoc assignments. Two different random post-hoc assignments were also tested and did not change the results shown in Fig. 4. Dunnett's test, utilized to analyze the simulated rescue experiment in Fig. 4D, was specifically designed to compare multiple intervention groups simultaneously with a single reference group (Dunnett, 1955). The null hypothesis of the test is that none of the intervention groups have a mean value significantly different from that of the reference group. The harmonic mean of the control ($n = 8$) and test ($n = 4$) sample sizes was 16/3; the mean squared error (MSE) calculated from the data shown in Fig. 4D was 0.013; the corresponding critical values from Dunnett's tables were $t_{critical} \approx 3.0$ at $\alpha = 0.05$ and $t_{critical} \approx 4.3$ at $\alpha = 0.01$.

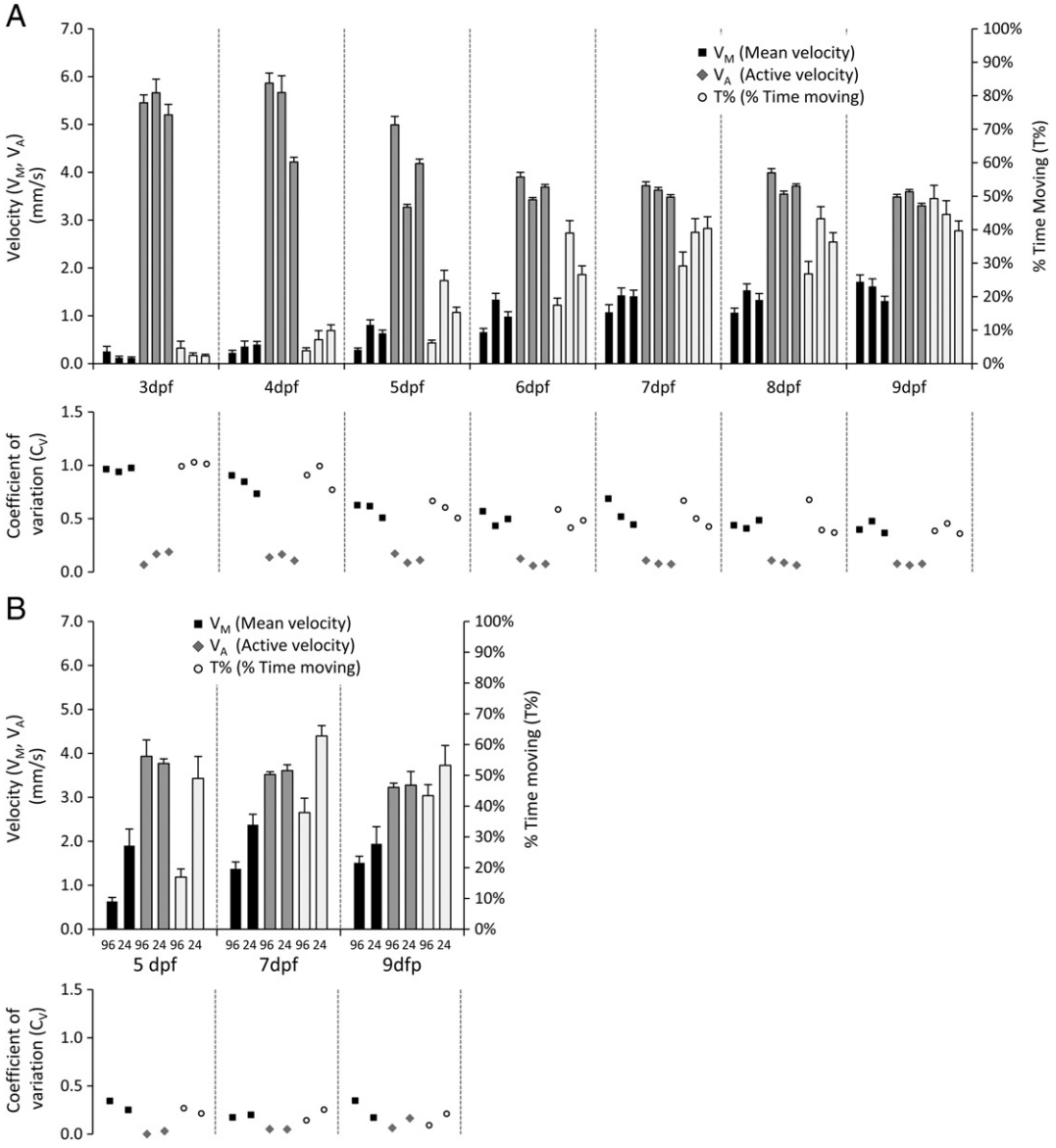

Fig. 1. Development of spontaneous propulsive movements in zebrafish larvae. A: The upper chart shows V_M, V_A and T% from three independent experimental replicates at each developmental time point 3–9 dpf. The scale for V_M and V_A is shown on the vertical axis to the left of the chart, and the scale for T% is shown at the right. Error bars show the standard error of the mean. The lower chart shows the coefficient of variation C_V, for each of the points shown above. B: The upper chart shows V_M, V_A and T% in larvae at 5, 7 or 9 dpf, recorded in either 96- or 24-well plates as indicated. Error bars show the standard error of the mean. The lower chart shows the coefficient of variation C_V, for each of the points shown above.

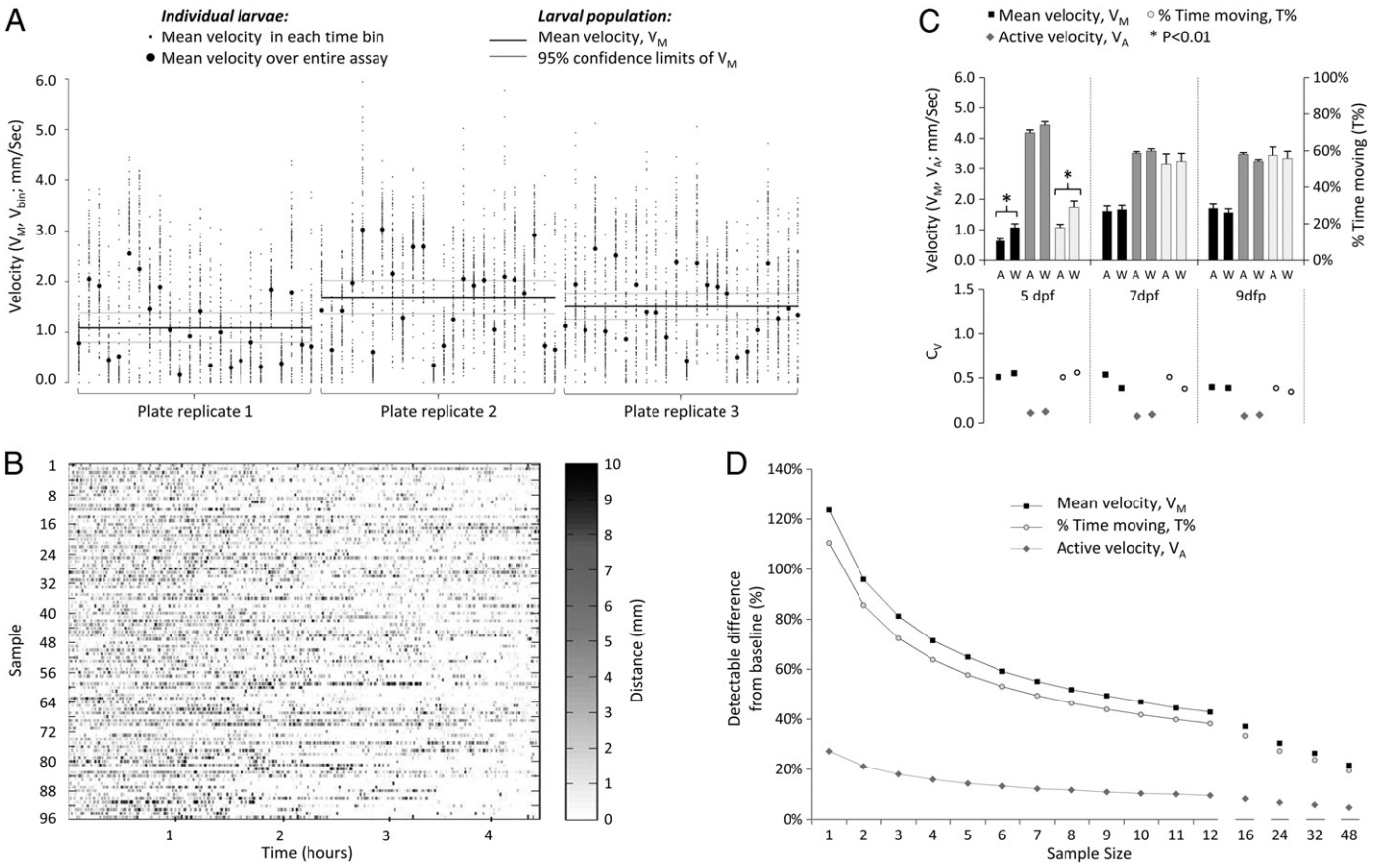

Fig. 2. Sources and consequences of variability in spontaneous movement. A: The graph shows details of three individual experimental replicates, in which spontaneous movements of 24 larvae were measured in 96-well plates for 4 h, at 7 dpf. The y-axis represents velocity; individual larvae are shown on the x-axis, grouped by experimental replicate. For each experimental replicate, the population mean and 95% confidence limits of the population mean over a 4-hour recording are shown as solid black and gray lines respectively, showing the variation in assay output between experiments. The mean velocity of each individual animal over the entire 4-hour recording is shown as a black circle, illustrating inter-larval variability. In order to demonstrate intra-larval variability, the recording was divided into 100 sequential time bins of equal duration; the mean velocity in each of these time bins is shown as a series of small points scattered around the individual larval mean for the whole recording. B: The figure shows the mean velocity of 96 larval zebrafish in 100 equal time bins over a 4.5 h recording. The x-axis shows time; individual larvae are shown on the y-axis. Each time/animal data point is shaded according to the amount of movement that occurred in the time bin, allowing comparison between the amount of movement made by each animal at any given time, and visual evaluation of trends over the course of the assay. C: The figure shows spontaneous movement of strain AB and strain WIK zebrafish at 5, 7 and 9 dpf. The upper chart illustrates V_M, V_A and T% and the lower chart shows C_V for each point in the upper chart. D: The graph shows a power analysis, in which larval sample size at 7 dpf is related to detectable differences in V_M, V_A and T% from baseline (expressed as % baseline values), assuming $\alpha = 0.05$ and $\beta = 0.9$.

Results

Development of spontaneous movement

Video recordings were made of wild-type strain AB zebrafish larvae between 3 and 9 days post-fertilization (dpf), moving spontaneously in trans-illuminated multiwell plates. Larvae were housed inside an incubator to regulate temperature and isolate the experiment from extraneous visual and auditory stimuli. Each sample consisted of 24 larvae. Three independent biological replicates for each time point were derived from different clutches of embryos and were recorded on different days.

The recordings were analyzed in order to measure spontaneous propulsive movements (Fig. 1A). Mean velocity (V_M = total larval displacement/time of recording) increased with age from 3 dpf (0.14 ± 0.02 mm/s, mean ± standard error) to 9 dpf (1.55 ± 0.08 mm/s). In contrast, active velocity (V_A = total displacement/time spent moving) decreased with age from 3 dpf (5.48 ± 0.10 mm/s) to 6 dpf (3.67 ± 0.04 mm/s), remaining approximately stable thereafter until 9 dpf (3.46 ± 0.03 mm/s). The increase of V_M with age, despite the decline in V_A, was explained by disproportionate growth in the percentage of time spent moving (T% = time spent moving/duration of recording), which steadily increased between 3 dpf (3.0 ± 0.31%) and 9 dpf (45.0 ± 2.0%). A transition between qualitative swimming patterns that underlie propulsive movements, from sporadic burst swimming (infrequent, high-velocity) to more mature beat-and-glide swimming (more continuous, slower), takes place between 4 and 6 dpf (Buss and Drapeau, 2001). This accounts for the measured changes in V_A, and T% at this developmental point.

Effect of well size on movement

One potential concern regarding measurement of propulsive movement in 96-well plates is that the small chamber size with respect to the size of the animal may introduce mechanical constraint artifacts. In order to address this possibility, we compared spontaneous movement measured in 96- and 24-well plates at 5, 7 and 9 dpf (Fig. 1B). The ratio of well size to larval length is significantly higher in 24-well plates than in 96-well plates (Supplementary Fig. 3). As expected, the larger wells were associated with more spontaneous displacement over a recording period (7 dpf, V_M in 96-well plate 1.5 ± 0.15 mm/s, 24-well 2.13 ± 0.22 mm/s, $p<0.01$). V_A was similar in 24-well and 96-well plates, whereas T% was higher in 24 well plates (7 dpf, 96-well 38 ± 3%, 24-well 63 ± 5%, $p<0.01$); this suggests that the constrained environment in 96-well plates reduced the frequency with which movements were made, but not their execution. Although larvae

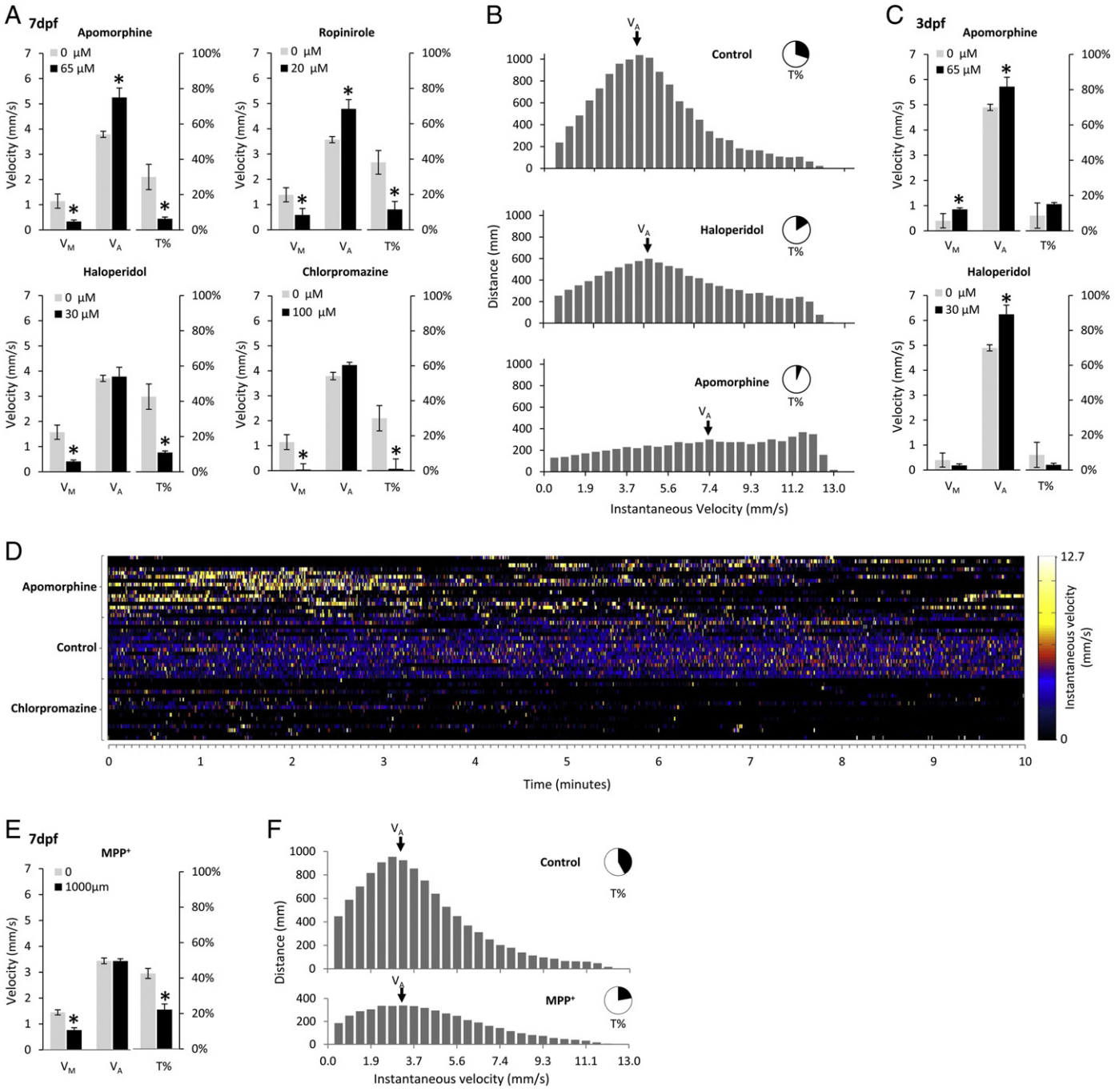

Fig. 3. Role of dopamine in regulating spontaneous movements. A: The four charts show the effects of two dopamine receptor agonists, apomorphine and ropinirole, and two dopamine receptor antagonists, haloperidol and chlorpromazine, on V_M, V_A and T% at 7 dpf. The concentrations of the drugs are shown in the chart; concentration–response curves for each drug are shown in Supplementary Fig. 3. The scale for V_M and V_A is shown on the vertical axis to the left of each chart, and the scale for T% is shown at the right. Error bars show the standard error of the mean. B: The three histograms show the distribution of instantaneous velocities of spontaneous movements that contributed to displacement of control (top), haloperidol (middle) or apomorphine (lower) exposed larvae. In each chart, the x-axis shows instantaneous velocities corresponding to measured movement between video frames. The y-axis shows the total amount of displacement in mm that occurred at that velocity over the duration of the assay. V_A is indicated in each chart, and the inset pie chart shows T%. C: The charts show the effects of a dopamine receptor agonist, apomorphine, and a dopamine receptor antagonist, haloperidol, on V_M, V_A and T% at 3 dpf. Axes and error bars are the same as panel A. D: The figure shows the instantaneous velocity of 48 larval zebrafish over 10 min of a recording. The x-axis shows time. The y-axis shows individual larvae, grouped by drug exposure (apomorphine, top 16 rows; control, middle 16 rows; chlorpromazine, lower 16 rows). Each time/animal data point is colored to depict instantaneous velocity according to the color scale shown to the right of the figure. E: The chart shows the effects of exposure to the dopaminergic neurotoxin MPP^+ on V_M, V_A and T% at 7 dpf. The scale for V_M and V_A is shown on the vertical axis to the left of the chart, and the scale for T% is shown at the right. Error bars show the standard error of the mean. F: The two histograms show the distribution of instantaneous velocities of spontaneous movements that contributed to displacement of control (top) or MPP^+-exposed (lower) larvae. In each chart, the x-axis shows instantaneous velocities corresponding to measured movement between video frames. The y-axis shows the total amount of displacement in mm that occurred at that velocity over the duration of the assay. V_A is indicated in each chart, and the inset pie chart shows T%.

showed increased spontaneous movement in 24-well plates, it is unlikely that this format will confer any advantage for screening purposes. The coefficient of variation for V_M, V_A and T% was similar between the plate sizes, and the larger number of wells in the 96-well plate format presents a fourfold throughput advantage, allowing larger samples sizes in each treatment group or a larger number of test conditions.

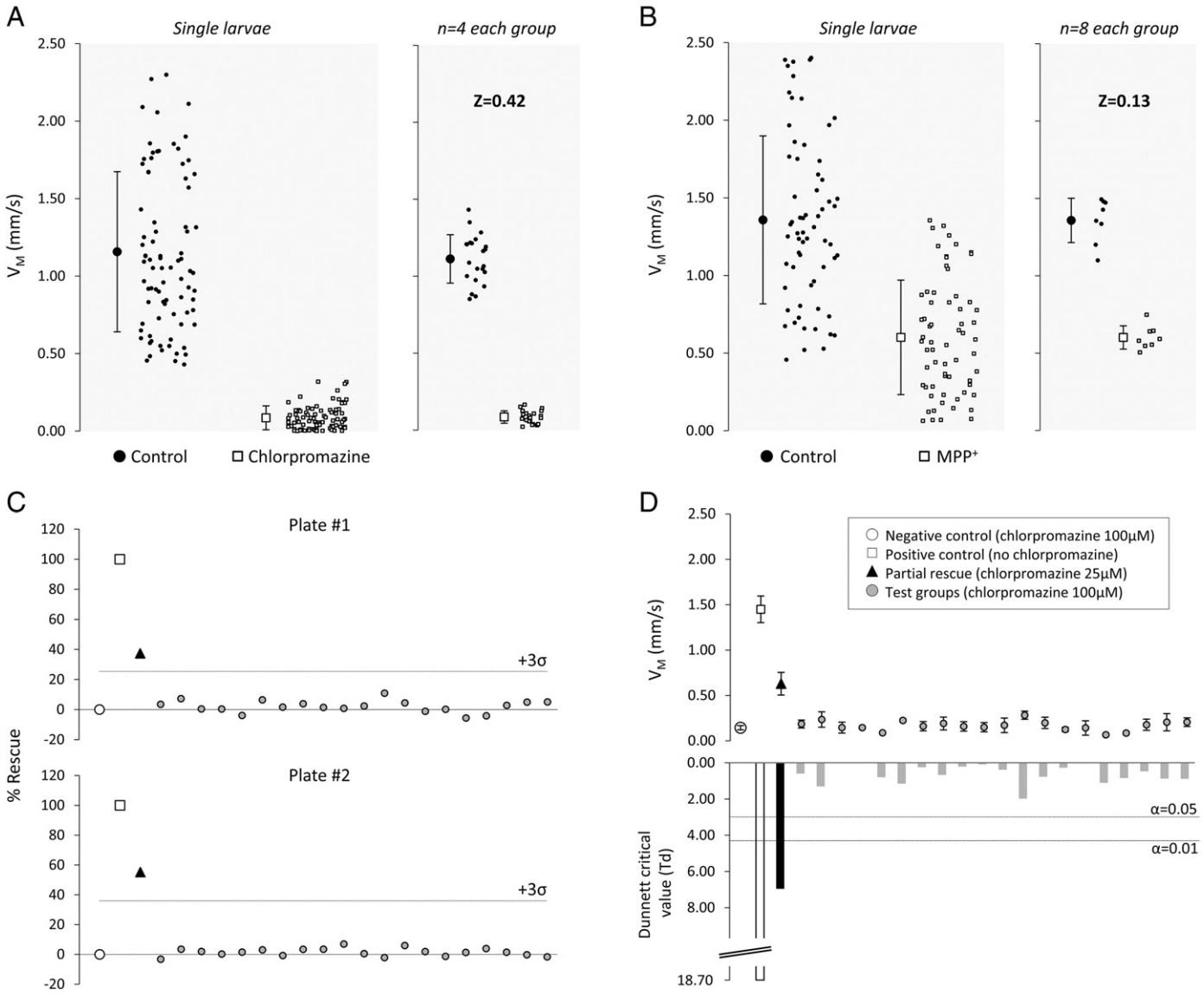

Fig. 4. V_M assay performance characteristics and implementation. A: The scatter plots show V_M measurements for controls (black circles) and larvae that were exposed to chlorpromazine (white squares). The left panel shows the distributions of measurements for individual larvae together with the sample means and standard deviations (84 larvae in each sample). The right panel shows the distributions of mean V_M for groups of four larvae, together with the sample means and standard deviations (21 groups of four larvae). B: The scatter plots show V_M measurements for controls (black circles) and larvae that were exposed to MPP^+ (white squares). The left panel shows the distributions of measurements for individual larvae together with the sample means and standard deviations (64 larvae in each sample). The right panel shows the distributions of mean V_M for groups of eight larvae, together with the sample means and standard deviations (8 groups of eight larvae). C: Two replicates of a simulated rescue experiment are shown, in which chlorpromazine was used to induce a hypokinetic phenotype that could be partially ameliorated by altering the concentration of the drug. Eight larvae were treated with 100 μM chlorpromazine (negative control group; open circles) and 4 larvae were not exposed to chlorpromazine (positive control group; open boxes) to define the assay dynamic range. 20 groups of four larvae were each treated with 100 μM chlorpromazine (test groups; gray circles), and a single group of four larvae was treated with 25 μM chlorpromazine (rescue group; black triangles) to mimic a situation in which one group of larvae showed partial rescue of a motor phenotype in response to a molecule from a library. V_M for each group was normalized to the controls and expressed as % rescue, calculated as: $\text{rescue}(\%) = 100 \times \frac{V_M(x) - V_M(neg)}{V_M(pos) - V_M(neg)}$, where $V_M(x)$ is the mean V_M of larvae in group x, and $V_M(pos)$ and $V_M(neg)$ represent mean V_M of wild-type larvae (positive control) and chlorpromazine-exposed hypokinetic larvae (negative control) respectively. The cut-off for defining a 'hit', 3 standard deviations above the plate mean (excluding the positive control), is indicated. D: The charts show analysis of the same data shown in the upper panel of Fig. 4C. The upper chart shows mean $V_M \pm$ standard error, for each group of larvae. Mean V_M for each group was compared with the negative control group, using Dunnett's test for multiple comparisons. The lower chart shows the Dunnett's critical value for each comparison with the control group. The thresholds for statistical significance at $\alpha = 0.05$ and $\alpha = 0.01$ are indicated.

Sources of variability

Variability is a limiting factor for screening assays. Together with the expected magnitude of the treatment effect, assay variability dictates the sample size necessary to detect interventions that modulate assay output (see Discussion). The variability of V_M decreased between 3 dpf ($C_V = 1.01$) and 7 dpf ($C_V = 0.55$); similar C_V values were observed for T% (3 dpf, $C_V = 1.05$; 7 dpf, $C_V = 0.53$), whereas V_A showed much less variation at both early (3 dpf, $C_V = 0.15$) and later (7 dpf, $C_V = 0.09$) developmental time points (Fig. 1A). Consequently, most of the variability in the total displacement, as measured by V_M, is accounted for by variability in the proportion of time spent moving, T%, rather than in the velocity of movements, V_A. We sought to establish whether any of the potential contributors to variability could be eliminated; three sources of variability in V_M were identified. First, the motor activity of individual zebrafish larvae showed significant alterations over the course of a recording (intra-larval variability; Fig. 2A). These changes in activity over time did not show discernable periodicity and were

asynchronous between larvae, suggesting that they did not occur in response to an extraneous environmental trigger (Fig. 2B). Second, the total amount of movement over an assay showed variation between larvae from the same population (inter-larval variability; Fig. 2A), even after recordings of several hours duration were analyzed to minimize intra-larval variability. Finally, experimental replicates yielded population means that differed from one another (inter-assay variability; Fig. 2A). Hierarchical analysis of variance showed that 98% of the overall variance of V_M was accounted for by intra- and inter-larval variability. This suggests that variability attributable to systematic inter-assay differences is small and that intrinsic larval factors determine most of the assay variability. Genetic background is well documented to influence behavioral performance in other systems and is a possible source of larval-intrinsic variability. Consequently, we asked whether spontaneous movement differed between two wild type zebrafish strains, AB and WIK (Johnson and Zon, 1999) (Fig. 2C). WIK larvae showed increased T% at 5 dpf (AB 15 ± 2%, WIK 25 ± 3%, $p = 0.0052$), resulting in an increased V_M (AB 0.64 ± 0.07 mm/s, WIK 1.08 ± 0.12 mm/s, $p = 0.0029$); the variances of these parameters were also statistically different between the strains at this time point (V_M $p = 0.005$, T% $p = 0.007$, F-test). At later developmental points, spontaneous movement was not different between AB and WIK larvae. These data are compatible with genetic heterogeneity being a contributor to inter-larval variability before 7 dpf. However the differences were relatively small and it is unclear whether attempting to reduce genetic variability by employment of less genetically heterogeneous zebrafish strains will be advantageous for these studies.

In the context of the measured variability, power analysis suggested that relatively small differences in motor behavior could be detected between manageable samples of larvae that had undergone different experimental manipulations (Fig. 2D), provided analysis was carried out after 5 dpf. For example, three experimental groups and a control group, each of 24 larvae, could be accommodated in a single 96-well plate. At 7 dpf this would allow detection of differences between control and experimental larvae of 30–35% in V_M and T%, and <10% in V_A, assuming $\beta = 0.9$ and $\alpha = 0.05$.

Role of dopamine

We next asked how dopaminergic function contributes to the regulation of spontaneous propulsive movements, by employing a pharmacological approach to manipulate dopamine signaling (Fig. 3A). Data shown in Fig. 3 are derived from experiments in which 24 strain AB larvae were analyzed in each experimental group. Three independent biological replicates, using larvae from different clutches recorded on different days, showed similar results for each experiment.

At 7 dpf, the dopamine receptor antagonists haloperidol and chlorpromazine showed little effect on V_A, but reduced T% considerably (control 42.6 ± 3.2%, 30 μM haloperidol 11.0 ± 0.7%, $p<0.001$; control 30.0 ± 2.9%, 100 μM chlorpromazine 1.0 ± 1.8%, N = 24, mean ± standard error), resulting in decreased V_M (control 1.57 ± 0.12 mm/s, 30 μM haloperidol 0.41 ± 0.03 mm/s, $p<0.001$; control 1.14 ± 0.12 mm/s; 100 μM chlorpromazine 0.04 ± 0.01 mm/s, $p<0.001$). Conversely, the dopamine receptor agonists apomorphine and ropinirole increased V_A (control 3.8 ± 0.05 mm/s, 65 μM apomorphine 5.3 ± 0.15 mm/s, $p<0.001$; control 3.57 ± 0.05 mm/s, 20 μM ropinirole 4.79 ± 0.15 mm/s, $p<0.001$). Both agents, however, strongly reduced T% (control 30 ± 3%, 65 μM apomorphine 6 ± 0.4%, $p<0.001$; control 38 ± 3%, 20 μM ropinirole 12 ± 2%, $p<0.001$), resulting in a decreased V_M (control 1.14 ± 0.12 mm/s, 65 μM apomorphine 0.34 ± 0.02 mm/s, $p<0.001$; control 1.38 ± 0.11 mm/s, 20 μm ropinirole 0.59 ± 0.1 mm/s, $p<0.001$). The effects of dopaminergic agents on V_A are illustrated in Fig. 3B. Under control conditions, movements at instantaneous velocities close to V_A accounted for most of the distance moved over the recording. Treatment with dopaminergic antagonists reduced the number of movements during the recording but not the shape of the velocity distribution accounting for larval displacement. In contrast, dopaminergic agonists modulated the distribution such that movements at high instantaneous velocity became relatively more frequent. The different effects of dopaminergic agonist and antagonist drugs on patterns of movement are illustrated graphically in Fig. 3D. Control larvae showed regular periods of movement at velocities close to V_A throughout the recording. Movements occurred much less frequently after chlorpromazine exposure, whereas apomorphine exposure gave rise to infrequent bursts of high-velocity movement.

As previously suggested (Thirumalai and Cline, 2008), the motor response to dopaminergic agents appeared to change around 5 dpf (Fig. 3C). In contrast to our observations at 7 dpf, at 3 dpf apomorphine increased V_M (control 0.40 ± 0.22, 65 μM apomorphine 0.85 ± 0.18, $p<0.001$) by effecting modest increments in both T% (control 8.65 ± 5%, 65 μM apomorphine 15.13 ± 3%, $p = 0.012$) and V_A (4.90 ± 0.45 mm/s, 65 μM apomorphine 5.72 ± 0.47 mm/s, $p = 0.005$). At 4 dpf, haloperidol increased V_A (control 4.90 ± 0.45 mm/s, 30 μM haloperidol 6.24 ± 0.65 mm/s, $p<0.001$) but reduced V_M (control 0.4 ± 0.22 mm/s, 30 μM haloperidol 0.18 ± 0.07 mm/s, $p = 0.032$) by causing a disproportionate decrease in T% (control 8.65 ± 5%, 30 μM haloperidol 2.94 ± 1.28%, $p = 0.013$). Assays to determine dopaminergic function by measuring spontaneous movement should be designed with this developmental change in mind.

We next asked whether similar changes in spontaneous movement resulted from disruption of endogenous dopamine function using a different approach to that shown in Figs. 3A–D. In zebrafish larvae, the neurotoxin MPP^+ causes a transient reduction in dopamine neuron count during development, associated with partial depletion of larval dopamine content (Sallinen et al., 2008). V_M was reduced in larvae exposed to MPP^+ (control 1.45 ± 0.10 mm/s, MPP^+ 0.76 ± 0.11 mm/s, $p<0.001$) (Fig. 3E). In agreement with our findings in larvae exposed to dopamine receptor antagonists, this decrease was attributable to a reduction in the proportion of time spent moving, T% (control 42.6 ± 0.10 mm/s, MPP^+ 22.1 ± 0.11 mm/s, $p<0.001$) rather than a reduction in active velocity, V_A (control 3.43 ± 0.09 mm/s, MPP^+ 3.44 ± 0.09 mm/s, $p = 0.95$). Consequently, the distributions of instantaneous velocities accounting for displacement of control and MPP^+-exposed animals were similar, whereas the lower total number of movements that occurred in MPP^+-exposed animals accounted for the reduced V_M. Together, these data suggest a role for endogenous dopamine in regulating the initiation of spontaneous movements, but not in their execution.

Spontaneous movement as a screening tool

We next tested whether measurement of spontaneous propulsive movement might be used as a discovery tool to identify alterations in dopaminergic signaling in a screen. Although V_A showed least variability of the three parameters we measured, it was unaffected by inhibiting endogenous dopamine function and is therefore unsuitable as an assay for this application. Robust changes in V_M and T% resulted from exposure to MPP^+ or dopamine receptor antagonist drugs. We evaluated V_M as a screening assay because this parameter is more likely than T% to be directly comparable between experimental systems (see Discussion and Supplementary data).

In order to define the assay window of V_M in different models we compared populations of control larvae at 7 dpf with animals exposed to chlorpromazine (large effect on V_M) or MPP^+ (more modest effect on V_M). As predicted, there was separation between the V_M distributions of individual control and chlorpromazine-treated larvae, whereas there was substantial overlap between individual V_M values of control and MPP^+-exposed larvae. For both of these models, the Z-factor (a numerical value that is defined by dynamic signal range and variability — see Discussion) was negative, suggesting that measurement of individual larval V_M values would be insufficiently robust for

screening purposes, as would be concluded intuitively from examining the population distributions in the left panels of Figs. 4A and B. The variability of V_M measurements was reduced by taking mean values of replicate samples; as expected, mean V_M values for groups of larvae also tended towards the mean of the original sample as the size of each group increased. At a sample size of $n = 4$ larvae in each group, robust separation of control and chlorpromazine-exposed groups of larvae was evident (Fig. 4A, right panel). Correspondingly, for $n = 4$ per data point, the Z-factor for control versus chlorpromazine-exposed animals was 0.42 suggesting that, by using 4 replicates of each treatment, V_M could be used as a robust readout to detect rescue of a model with a severe motor phenotype (Zhang et al., 1999). For the relatively subtle motor phenotype resulting from MPP^+exposure, it was necessary to analyze larger groups of replicates in order to separate MPP^+- exposed and non-exposed populations with sufficient rigor for the assay to be valuable for screening. At a sample size of $n = 8$ larvae per group, the Z-factor was 0.13, suggesting that a practicable number of well replicates would allow use of V_M as a phenotypic assay to detect rescue of even the relatively mild abnormality induced by MPP^+.

Finally, we asked how a small molecule discovery effort utilizing V_M might be executed in practice. It is standard procedure to include positive and negative controls on each plate of a screening assay to ensure assay quality control. In the case of spontaneous movement, this is especially important since the assay is variable from replicate to replicate (Figs. 1A and 2A). Consequently, changes in V_M must be interpreted with respect to controls, for example by relating each data point to the assay dynamic range (as defined by the positive and negative controls). This standardization allows comparison between assays carried out on different days. An example is shown in Fig. 4C. In this experiment, designed to simulate a screening assay, 8 negative control larvae were exposed to 100 μM chlorpromazine in order to induce a hypokinetic phenotype and 4 vehicle-treated wild-type animals with normal movement represent positive controls. The remainder of each plate contained 21 groups of 4 larvae each. Larvae in 20 of these groups were treated with 100 μM chlorpromazine to mimic the effects of compounds that did not rescue the motor phenotype. The remaining group was treated with 25 μM chlorpromazine to mimic incomplete amelioration of the hypokinetic phenotype, as might be observed if an unknown compound caused partial rescue of function. The two different assays were normalized as described above, allowing direct comparison between these replicate experiments.

As expected, the rescue group showed higher mean V_M than the other test groups. The % rescue varied between assays, and the test groups showed variability with respect to the controls. There are no generally accepted criteria for selecting 'hits' in a screening assay. Arbitrary cut-off points for selection are frequently used, including: assay result differs from the plate mean by a certain multiple of the standard deviation (Z-score); assay result is in the top few % of readings; or assay result exceeds a predetermined threshold % of the positive control; and selection of hits is often influenced by other factors such as capacity for secondary assays, cost and past experience (Malo et al., 2006). In the example shown in Fig. 4C, the partial rescue group would be identified as a hit in both replicates by the criterion that its mean V_M is >3 standard deviations greater than the plate mean (i.e. Z-score >3), which would be a reasonable and commonly used outcome measure (Malo et al., 2006). The inclusion of replicates for each data point provides an additional possibility, since each data point is itself now comprised of a sample, such that it is possible to calculate the confidence with which the mean V_M for each test compound differs from the control mean. In panel 4D, the data from plate #1 in panel 4C were analyzed using Dunnett's test for multiple comparisons (Dunnett, 1955), in order to compare V_M between each of the test or rescue groups and a single reference population (in this case the negative control group). In this analysis, only the positive control and partial rescue groups showed a highly statistically significant difference from the negative control group (Dunnett's critical value exceeded the $\alpha = 0.01$ threshold). These data suggest that a shared-control statistical design might be employed in addition to traditional screening assay metrics to identify interventions that ameliorate motor phenotypes, without necessarily effecting complete rescue.

Discussion

Two general strategies have been employed to quantify zebrafish larval movement from video recordings. The first involves quantification of pixels whose value changes in consecutive frames, by subtraction of pixel gray scale values, or counting pixels whose binary value changes. Quantification of pixel change gives an indication of larval activity, since more movement in the image is associated with a larger number of pixels changing from frame to frame. This method does not involve identification of individual larvae and consequently can be carried out in situations where more than one animal is moving within the same field of activity. A pixel quantification method has been used highly effectively in a chemical screen to monitor patterns of activity in response to ambient illumination, allowing detection of characteristic responses following exposure to compounds with shared neuropharmacological actions (Rihel et al., 2010). Depending on video recording parameters, however, this approach can be insensitive to velocity of movement, because a frame-to-frame larval displacement to a new position outside the original larval outline would cause maximal pixel change regardless of the magnitude of displacement. In addition, the reported output (summed pixel value changes/frame) has an indirect relationship to larval kinetic properties and its magnitude could be influenced by larval size, pigmentation, illumination and hardware details.

The second method for quantification of larval movement involves tracking the locations of individual larvae, allowing calculation of displacement and velocity. This method is currently only reliable when a single animal is moving within a field of observation, since unequivocal identification of animals following overlap/collision events has not yet been resolved. A multiwell plate can house individual larvae separately, allowing reliable identification and tracking of up to 96 animals simultaneously. Tracking is not sensitive to movements that do not alter the location of the larval centroid, for example rotations or some changes in shape. However, we favored the tracking method for the present application for three reasons. First, resolution of velocity would allow us to measure directly whether loss of dopaminergic function caused slowness of movement, paucity of movement, or both. Second, the output of this type of analysis should facilitate comparison between data sets, since V_M is calculated from two directly determined physical properties (displacement, time) and consequently is influenced most strongly by the kinetic behavior of zebrafish larvae rather than the method used for measurement. Finally, the measurement of a continuous kinetic variable should allow quantitative analysis, permitting identification of partial rescue of Parkinsonian mutants.

In contrast to V_M, which was directly measured, its components V_A and T% were derived after identifying video frames that did not contribute to overall displacement. This process is dependent on threshold criteria for distinguishing stochastic pixel noise from movement, allowing the categorical assignment of video frames as showing movement or no movement of an individual larva from the previous frame. Optimization of video capture and displacement thresholds for T% and V_A calculations are discussed in Supplementary data. At the video frame rate used in this study, V_A is only an estimate of larval velocity during movement, because peak larval velocities are attained only transiently and therefore can only be captured using high frame rate recordings. Despite this potential limitation, we observed V_A and T% changing independently during development in a pattern consistent with the previously reported developmental transition in swimming patterns. We were also able to make some

interesting observations regarding pharmacologically-evoked changes in spontaneous movements.

Dopamine receptor antagonists and the dopaminergic neurotoxin MPP^+ reduced the proportion of video frames in which larvae had moved from the previous frame (T%) but did not alter the mean amount (V_A) or distribution of frame-to-frame displacement when movement occurred. We interpret these findings as showing that reduced spontaneous larval movement following disruption of dopamine signaling was attributable to a decrease in the number of movements executed, rather than alterations in individual propulsive movements. This suggests that discrete mechanisms underlie decisions to move and the performance of movements, compatible with a model in which convergent influences (including the dopaminergic system) regulate activation of a central pattern generator that produces stereotyped neural signals mediating propulsion.

The pharmacological properties of the dopamine receptor agonists and antagonists used in this study were determined in mammalian systems. There is some sequence divergence between mammalian dopamine receptors and their zebrafish paralogs, raising the possibility that the effects seen here are attributable to drug actions at other types of receptor. However, we observed a similar pattern of changes in motor activity in response to two structurally distinct (phenothiazine and butyrophenone) dopamine receptor antagonists. These changes were similar to those observed after exposure to the dopaminergic neurotoxin MPP^+, which impairs dopaminergic neurotransmission by destruction of presynaptic dopamine terminals rather than modulation of dopamine receptor activation. Consequently, although we have not formally proven that the observed phenotypes were attributable to modulation of endogenous dopaminergic function, this remains the most parsimonious explanation for the observed changes. Further studies, such as binding assays to determine the receptors for these agents in the zebrafish, or genetic ablation studies to selectively target dopaminergic neurons, may be necessary to fully clarify this issue.

The major objective of this study was to establish a simple assay that could be applied to high-throughput genetic and chemical modifier screens in zebrafish models of Parkinsonism and other movement disorders. Exposure to dopamine receptor antagonists or a dopaminergic neurotoxin caused robust changes in movement, such that differences attributable to experimental interventions could be detected above assay noise robustly in small samples. However, utility as a drug discovery tool requires more robust assay metrics than those necessary to define significant differences between populations. A screening window coefficient, the Z-factor, which is determined by the variability and dynamic signal range of an assay, is often used to assess the quality of assays for screening applications (Zhang et al., 1999). The Z-factor is a dimensionless, numerical value that describes the degree of separation between [mean + 3SD] of a negative control population, and [mean − 3SD] of a positive control population (for a normal distribution mean ± 3SD encompasses approximately 99% of the population). The Z-factor can assume any value <1. A Z-factor approaching 1 denotes an ideal case of wide separation and little variability; a Z-factor >0 denotes separation between the means ± 3SD of the positive and negative control. Based on these considerations, Zhang et al. (1999) suggested that assays should be classified as "excellent" ($Z>0.5$), "doable" ($0.5 \geq Z>0$), "yes-no type" ($Z=0$), and "screening essentially impossible" ($Z<0$), and this system has been widely adopted by the high-throughput screening community. If the standard deviation of positive and negative control values is equal, a Z-factor of 0 represents separation between the positive and negative control means by 6 standard deviations. These criteria are highly conservative, necessitated by the potential for inferior assays to generate abundant false positive and false negative results in large-scale high-throughput screens.

While biochemical assays routinely achieve Z-factors of >0.5, complex cellular assays, siRNA assays and whole organism assays often do not reach this level of performance due to their inherently larger biological variability and more limited dynamic signal range. However, the immensely rich biology of in vivo assays suggests that they have high value despite this potential limitation. For example, the recapitulation of disease pathogenesis in a representative system in vivo may offer opportunities to discover genes or compounds that act through cell non-autonomous mechanisms. Furthermore, in vivo models may have particular value for drug discovery applications when pharmacological targets are unknown, as is true for neurodegenerative disease. In this case, lack of knowledge regarding molecular pathogenesis precludes the development of meaningful simpler biochemical assays. Cellular and in vivo assays can be improved by the use of replicates to reduce variability, with the added advantage that loading and toxicity artifacts are also essentially eliminated. Consistent with our recent experience in a zebrafish angiogenesis assay (Vogt et al., 2009), we found that the use of replicates boosted V_M assay performance to a level allowing reliable detection of positives using a Z-score criterion of >3 . For a model with a severe motor phenotype (exemplified by chlorpromazine exposure), replicate sizes of 4 were sufficient for the Z-factor to approach the 0.5 threshold for the assay to be judged as excellent, similar to the standards routinely achieved by simple biochemical measurements. Even in the case of a milder motor phenotype (exemplified by MPP^+ toxicity), replicate sizes of 8 were sufficient to ensure that the assay performed adequately for screening. These replicate sizes are practicable, as shown by a recent zebrafish phenotype-based chemical screen using replicate sizes of 8, in which a library of 3968 compounds was analyzed for molecules that effected changes in motor activity in response to light–dark cycling (Rihel et al., 2010). The assay used in the published screen was relatively complex; recordings were made over three days and analyzed to identify patterns of behavioral alteration. This suggests that similar replicate sizes using a simpler assay, measurement of V_M, should allow the interrogation of small molecule libraries for agents that rescue a Parkinsonian phenotype.

Stable genetic zebrafish models of Parkinsonism are still under development, and the severity and variability of their motor phenotypes will dictate whether they can be subjected to small molecule or genetic discovery efforts using this approach. If, at larval time points amenable to screening, these models develop significant and reproducible hypokinesia (similar or greater in magnitude to the movement abnormalities we observed after MPP^+ exposure), a manageable replicate size would allow reliable detection of a compound or genetic mutation that partially rescued motor function. Using the shared-control design we utilized in Figs. 4C and D, a single experimental apparatus would allow >1000 compounds to be tested at multiple concentrations within a few months. Detailed reports of stable genetic zebrafish models of Parkinsonism are therefore awaited with considerable interest to determine whether their phenotypes will be suitable for this kind of analysis.

Acknowledgments

This work was funded by research grants from: NIH (NS058369 and HD053287); the Pittsburgh Foundation (M2005-0071); the Society for Progressive Supranuclear Palsy (468–08); and the RIMED Foundation. CM is a RIMED scholar.

Appendix A. Supplementary data

Supplementary data to this article can be found online at doi:10.1016/j.nbd.2011.05.016.

References

Bandmann, O., Burton, E.A., 2010. Genetic zebrafish models of neurodegenerative diseases. Neurobiol. Dis. 40, 58–65.

Bretaud, S., et al., 2004. Sensitivity of zebrafish to environmental toxins implicated in Parkinson's disease. Neurotoxicol. Teratol. 26, 857–864.

Buss, R.R., Drapeau, P., 2001. Synaptic drive to motoneurons during fictive swimming in the developing zebrafish. J. Neurophysiol. 86, 197–210.
Cario, C.L., Farrell, T.C., Milanese, C., Burton, E.A., 2011. Automated measurement of zebrafish larval movement. J. Physiol. Jun 6 [Epub ahead of print].
Drapeau, P., et al., 2002. Development of the locomotor network in zebrafish. Prog. Neurobiol. 68, 85–111.
Dunnett, C.W., 1955. A multiple comparison procedure for comparing several treatments with a control. J. Am. Stat. Assoc. 50, 1096–1121.
Giacomini, N.J., et al., 2006. Antipsychotics produce locomotor impairment in larval zebrafish. Neurotoxicol. Teratol. 28, 245–250.
Johnson, S.L., Zon, L.I., 1999. Genetic backgrounds and some standard stocks and strains used in zebrafish developmental biology and genetics. Methods Cell Biol. 60, 357–359.
Kokel, D., et al., 2010. Rapid behavior-based identification of neuroactive small molecules in the zebrafish. Nat. Chem. Biol. 6, 231–237.
Lam, C.S., et al., 2005. Zebrafish embryos are susceptible to the dopaminergic neurotoxin MPTP. Eur. J. Neurosci. 21, 1758–1762.
Malo, N., et al., 2006. Statistical practice in high-throughput screening data analysis. Nat. Biotechnol. 24, 167–175.
McKinley, E.T., et al., 2005. Neuroprotection of MPTP-induced toxicity in zebrafish dopaminergic neurons. Brain Res. Mol. Brain Res. 141, 128–137.
Muto, A., et al., 2005. Forward genetic analysis of visual behavior in zebrafish. PLos Genet. 1, e66.
Orger, M.B., et al., 2004. Behavioral screening assays in zebrafish. Methods Cell Biol. 77, 53–68.
Panula, P., et al., 2010. The comparative neuroanatomy and neurochemistry of zebrafish CNS systems of relevance to human neuropsychiatric diseases. Neurobiol. Dis. 40, 46–57.
Peng, J., et al., 2009. Ethanol-modulated camouflage response screen in zebrafish uncovers a novel role for cAMP and extracellular signal-regulated kinase signaling in behavioral sensitivity to ethanol. J. Neurosci. 29, 8408–8418.
Rihel, J., et al., 2010. Zebrafish behavioral profiling links drugs to biological targets and rest/wake regulation. Science 327, 348–351.
Sallinen, V., et al., 2008. MPTP and MPP^+ target specific aminergic cell populations in larval zebrafish. J. Neurochem. 108, 719–731.
Tanabe, L.M., et al., 2009. Primary dystonia: molecules and mechanisms. Nat. Rev. Neurol. 5, 598–609.
Thirumalai, V., Cline, H.T., 2008. Endogenous dopamine suppresses initiation of swimming in prefeeding zebrafish larvae. J. Neurophysiol. 100, 1635–1648.
Vogt, A., et al., 2009. Automated image-based phenotypic analysis in zebrafish embryos. Dev. Dyn. 238, 656–663.
Zhang, J.H., et al., 1999. A simple statistical parameter for use in evaluation and validation of high throughput screening assays. J. Biomol. Screen. 4, 67–73.
Zon, L.I., Peterson, R.T., 2005. In vivo drug discovery in the zebrafish. Nat. Rev. Drug Discov. 4, 35–44.